

1 **Missing earthquake data reconstruction in the**
2 **space-time-magnitude domain**

3 **Angela Stallone^{1*}, and Giuseppe Falcone¹**

4 ¹Istituto Nazionale di Geofisica e Vulcanologia (INGV)

5 **Key Points:**

- 6 • A new Python toolbox for the replenishment of incomplete seismic catalogs is de-
7 veloped
8 • The code is freely-available, data-driven and minimizes the users' inputs
9 • Numerical and real-case tests are provided

*Via di Vigna Murata, 605 - 00143 Rome, Italy

Corresponding author: Angela Stallone, angela.stallone@ingv.it

Abstract

Short term aftershock incompleteness (STAI) can strongly bias any analysis built on the assumption that seismic catalogs have a complete record of events. Despite several attempts to tackle this issue, we are far from trusting any dataset in the immediate future of a large shock occurrence. Here we introduce RESTORE (REal catalogs STOchastic REplenishment), a Python toolbox implementing a stochastic gap-filling method, which automatically detects the STAI gaps and reconstructs the missing events in the space-time-magnitude domain. The algorithm is based on empirical earthquake properties and relies on a minimal number of assumptions about the data. Through a numerical test, we show that RESTORE returns an accurate estimation of the number of missed events and correctly reconstructs their magnitude, location and occurrence time. We also conduct a real-case test, by applying the algorithm to the M_W 6.2 Amatrice aftershocks sequence. The STAI-induced gaps are filled and missed earthquakes are restored in a way which is consistent with data. RESTORE, which is made freely available, is a powerful tool to tackle the STAI issue, and will hopefully help to implement more robust analyses for advancing operational earthquake forecasting and seismic hazard assessment.

1 Introduction

It is well known that analyzing an incomplete seismic catalog could severely bias studies aimed to: 1) estimate the Gutenberg-Richter parameters, their uncertainty, together with their variation in space and/or time (e.g. Knopoff et al., 1982; Schorlemmer et al., 2003; Woessner & Wiemer, 2005; Mignan & Woessner, 2012b; Marzocchi et al., 2020); 2) estimate the Epidemic-Type Aftershock Sequence (ETAS model: Ogata, 1988, 1998) parameters by maximum-likelihood techniques (Helmstetter et al., 2005, 2006; Hainzl et al., 2013; Omi et al., 2014; Seif et al., 2017; Zhuang et al., 2017); 3) perform a statistical analysis of earthquake data (e.g. Helmstetter et al., 2006; Christophersen & Smith, 2008; Iwata, 2008; Brodsky, 2011; Felzer et al., 2015; Stallone & Marzocchi, 2019). The first two types of studies, in particular, have application in operational earthquake forecasting and seismic hazard assessment (Woessner et al., 2015), this implying that complete recording of seismic events is of primary importance in any analysis of this kind. Unfortunately, a careful estimation of the magnitude of completeness M_c is a necessary but not sufficient condition for a robust seismicity analysis. As a matter of fact, temporal changes in M_c can occur, mainly due to short term aftershock incompleteness (STAI from now on) (Ogata & Katsura, 1993; Kagan, 2004; Mignan & Woessner, 2012b; Omi et al., 2013), which arise from the under-reporting of small events after large earthquakes. These fluctuations, although transient, can severely alter the final results. For instance, (Zhuang et al., 2017) demonstrate how severe can be the influence of short-term missing aftershocks on the estimation of the ETAS parameter α (which is linked to earthquakes triggering capability). A solution to this issue would be improving the detection of early aftershocks of a large earthquake. This is possible by implementing waveform-based techniques (Peng et al., 2006, 2007; Enescu et al., 2007, 2009; Peng & Zhao, 2009). However, even in these cases, the detection capability of the missing events is far from being optimal. A quick fix could be to draw out earthquakes occurred after a large shock, for as long as the time required to the magnitude of completeness to return to the average value estimated for the whole catalog. Alternatively, one could model the magnitude of completeness as a function of time $M_c(t)$ and keep only those events whose magnitude is $\geq M_c(t)$ (e.g. Helmstetter et al., 2006; Lippiello et al., 2012). However, these approaches are not trivial, since they rely on user-defined criteria for identifying the critical events to be removed. Furthermore, a cut-and-run strategy could yield to a severe diminishment of the analyzed data, which is not always desirable. More recently, (Zhuang et al., 2017, 2019) have proposed a stochastic algorithm to replenish the portions of a seismic catalog where smaller events are missing. This approach is based on empirical distribution functions that approximately describe the time-magnitude range of data where the catalog is assumed to be complete. Furthermore, it cannot be easily extended to the

63 spatial domain and the detection of the area where the record is incomplete is based on
 64 visual inspection. Here we present RESTORE, a Python toolbox based on a stochastic
 65 gap-filling method, which reconstructs missing events in the space-time-magnitude do-
 66 main and implements an automatized recognition of the critical regions with missing events
 67 (no input required from the user). RESTORE is built on well-known empirical proper-
 68 ties of earthquake data and relies on a fully data-driven approach, which severely min-
 69 imizes the number of assumptions and approximations about the data.

70 2 The algorithm

71 RESTORE (REal catalogs STOchastic REplenishment) allows to generate time,
 72 location and magnitude of those earthquakes that have not been detected by the seis-
 73 mic network due to the overlap of earthquake signals in seismic records after the occur-
 74 rence of a large earthquake. Given the transient characteristic of STAI, the replenish-
 75 ment of missing data only pertains to limited portions of the catalog, i.e. those being
 76 affected by the occurrence of a large event. First, the temporal variability of M_c is as-
 77 sessed by means of a sliding overlapping windows approach, which collects estimates of
 78 M_c at the end of each window. Since the window has a fixed number of events k and its
 79 shift δk is constant, estimates of M_c are elapsed by δk events. The algorithm implements
 80 a statistic-based approach to pinpoint those time intervals where a threshold value for
 81 the magnitude of completeness M_c^* is significantly exceeded ("STAI gaps" from now on).
 82 For each interval, fluctuations in the completeness magnitude, represented by the δk -shifted
 83 moving-window estimates of M_c , are accounted for to reconstruct the missing earthquakes:
 84 the higher the estimated M_c , the higher the number of earthquakes to be replenished.
 85 It follows that the moving-window approach is functional for both the identification of
 86 STAI gaps and for their discretization. The latter is essential for a high-resolution tem-
 87 poral reconstruction of M_c inside the STAI gaps. The algorithm evaluates, for each mag-
 88 nitude bin in each step, the difference between the observed counts and the counts pre-
 89 dicted by the Gutenberg-Richter relationship. This approach returns the simultaneous
 90 estimation of both the number and magnitudes of missing events at the bin level: the
 91 first is derived from the difference between observed and estimated counts, whereas the
 92 second is derived from the magnitude value in the bin. Occurrence time and location of
 93 the simulated events are reconstructed implementing Monte Carlo sampling techniques
 94 (inverse method, (Devroye, 1986)). More specifically, occurrence times are simulated from
 95 an uniform distribution whose support are the time limits of the δk -step. The latter is
 96 based on the assumption that earthquake detection rate can be assumed constant within
 97 intervals including few events, i.e within very short time intervals. In other words, the
 98 probability of missing events within a δk -step can be considered time-independent if the
 99 step width is much shorter than the whole STAI gap width. As regards the spatial in-
 100 formation, latitude and longitude of missing events are assigned with a probability that
 101 increases as the average rate of earthquake increases, the latter being derived from a Gaus-
 102 sian smoothing kernel. In the following, we examine the algorithm steps in more detail.

103 2.1 Query user inputs

104 The user is required to load the catalog as a csv file, in ZMAP format (i.e., Lon-
 105 gitude, Latitude, Year, Month, Day, Magnitude, Depth, Hour, Minute, Second). Alter-
 106 natively, he/she can download it from web services based on FDSN specification, by pro-
 107 viding the parameters listed in Table 1, left column. There are two main requirements
 108 for the correct implementation of RESTORE. First, the magnitude type in the seismic
 109 catalog must be the moment magnitude M_w (a bin size of 0.1 is assumed by default).
 110 This is required since magnitude scales other than the moment magnitude are inappro-
 111 priate for rigorous statistical analyses (Kagan, 2013). Second, the catalog should include
 112 a period of seismic quiescence before the onset of one or more relatively strong seismic
 113 sequences. This is necessary for the estimation of the reference value for the magnitude

Table 1. RESTORE input parameters^a.

CATALOG PARAMETERS (optional)	INPUT PARAMETERS
Minimum magnitude	Moving-window size
Minimum longitude	Moving-window step
Maximum longitude	Spatial map domain limits
Minimum latitude	t_{seq}
Maximum latitude	b -value
Maximum depth	α (Lilliefors test)
t_{start}	
t_{end}	

^aLeft: catalog parameters (to be provided only when downloading the catalog from web services based on FDSN specification) - t_{start} : string representing the start time of the catalog in a recognizably valid format; t_{end} : string representing the end time of the catalog in a recognizably valid format.

Right: RESTORE parameters - t_{seq} : starting time of the seismic sequence (i.e., end of the seismic quiescent period).

114 of completeness (M_c^*), which must not be affected by STAI. The parameters that need
 115 to be set for running RESTORE are reported in Table 1, right column. They will be ex-
 116 plained in more detail in the subsequent sections.

117 2.2 Reference value for the magnitude of completeness

118 The reference value M_c^* must be evaluated for the seismically quiescent period pre-
 119 ceding the onset of one or more relatively strong seismic sequences. By default, it is es-
 120 timated as the first magnitude value such that the hypothesis of exponentially-distributed
 121 data cannot be rejected at a significance level α (Lilliefors test, Lilliefors, 1969; Clauset
 122 et al., 2009). Alternatively, the user could input his/her own value for M_c^* , based on a
 123 priori information. RESTORE relies on *Mc-Lilliefors*, a Python routine which returns
 124 a robust and rigorous estimation of the magnitude of completeness by the Lilliefors test
 125 (Herrmann & Marzocchi, 2020b, 2020a). From now on, we always mean that the mag-
 126 nitude of completeness estimation has been performed by the *Mc-Lilliefors* routine.

127 2.3 Temporal variations in M_c

128 RESTORE implements a moving window approach to analyze the variation of the
 129 magnitude of completeness as a function of time. By default, the window size is $k = 1000$
 130 events (following Mignan & Woessner, 2012a), but it could be increased or decreased,
 131 depending on both the catalog size and the resolution the user needs to achieve. Intu-
 132 itively, a small window highlights short-term variation in M_c , but it could return a bi-
 133 ased estimate of M_c if the sample size is too small (due to the decreased power of the
 134 Lilliefors test); on the contrary, a larger window returns a faster and more robust esti-
 135 mate of M_c , but it is less sensitive to its transient fluctuations. The window is shifted
 136 by a step of δk events. By default, $\delta k = 250$ (following Mignan & Woessner, 2012a).
 137 The same considerations made for a larger/smaller window apply for a larger/smaller
 138 step. M_c is estimated and its values are collected at the end of each window. Since the
 139 window has a fixed number of events k and its shift δk is constant, estimates of M_c are
 140 elapsed by δk events.

141

2.4 Automatic detection of STAI gaps

142

143

144

145

146

147

148

149

150

151

STAI gaps are identified as those where $M_c \geq M_c^* + 2\sigma$, i.e. where M_c is significantly larger than the reference value. The bootstrap method (Efron, 1992) is implemented to estimate the uncertainty σ about the estimate of M_c^* returned by the Lilliefors test. Specifically, σ is obtained from 200 bootstrap samples, as suggested in (Woessner & Wiemer, 2005). The onset time of each gap is set equal to the time of the largest earthquake in the first step. Intuitively, it is the one responsible for the raise of the magnitude of completeness among the δk events. The end time of each gap is coincident with the occurrence time of the last event in the last step. In order to account for statistical fluctuations of the magnitude of completeness, small gaps - defined as those with a number of events $< 2 * \delta k$ - are removed.

152

2.5 Simulation of missing earthquakes

153

154

RESTORE implements a multi-scale approach for addressing the inherent problem of multidimensionality of the seismic process:

155

156

157

158

159

- Small scale: magnitude bin-level estimation of the number and magnitudes of missing events (Section 2.5.1);
- Medium scale: step-level estimation of the occurrence times of missing events (Section 2.5.2);
- Coarse scale: STAI gap-level simulation of missing events epicenters (Section 2.5.3).

160

2.5.1 Simulation of number of missing events and magnitudes

For a given STAI gap, the algorithm stores as many M_c estimates as the number of δk -steps in the gap. This information is used to evaluate the number of expected events at the magnitude bin level by means of the following equation, which relies on the Gutenberg-Richter frequency-magnitude relationship (we refer to Appendix 1 for its derivation):

$$N(M \geq M_{LB}) = N(M \geq M_{UB}) \cdot 10^{b \cdot mbin}, \quad (1)$$

where: 1) M_{LB} (M_{UB}) is the lower (upper) bound of the magnitude bin $mbin$, with $mbin = 0.1$ by default; 2) $N(M \geq M_{LB})$ is the expected number of events with magnitude $M \geq M_{LB}$; 3) $N(M \geq M_{UB})$ is the observed number of events with magnitude $M \geq M_{UB}$. Equation 1 allows to extrapolate the expected number of events with magnitude $M \geq M_{LB}$, given the complete recording of events at magnitudes $M \geq M_{UB}$. It is then straightforward to retrieve, for each bin, the expected number of events with magnitudes $M = M_{LB}$ ($M_{LB} \leq M < M_{UB}$), given the complete recording of events at magnitudes $M \geq M_{UB}$:

$$\begin{aligned} N(M = M_{LB}) &= N(M \geq M_{LB}) - N(M \geq M_{UB}) \\ &= N(M \geq M_{UB}) \cdot 10^{b \cdot mbin} - N(M \geq M_{UB}) \end{aligned} \quad (2)$$

161

162

163

164

165

166

167

168

169

170

Finally, the number of missing events in the bin is derived from the difference between the expected number of events in the bin, $N(M = M_{LB})$, and the observed number of events in the bin. RESTORE recursively implements Equation 1 and Equation 2 in order to estimate the number and magnitudes of missing events for all the bins between M_c^* - the reference value for the magnitude of completeness - and M_c^S , the magnitude of completeness estimated within the step. The algorithm starts at the bin whose upper bound is M_c^S : since magnitudes in the step are complete above M_c^S , Equation 1 and Equation 2 are implemented for the estimation of the number of missing events in the preceding bin. Then, variables are updated and the algorithm proceeds with the next preceding bin, following the recursive approach explained in Algorithm 1.

Algorithm 1: Magnitude simulation

```

1 for each STAI gap do
2   for each step in the gap do
3      $M_{UB} = M_c^*$ ;
4      $M_{LB} = M_{UB} - mbin$ ;
5      $N(M \geq M_{UB}) \rightarrow$  Counts of  $M \geq M_{UB}$  in the step
6     for each bin in the step do
7        $N(M \geq M_{LB}) = N(M \geq M_{UB}) \cdot 10^{b \cdot mbin}$ 
8        $N(M = M_{LB}) = N(M \geq M_{LB}) - N(M \geq M_{UB}) \rightarrow$  Expected
9       number of magnitudes in the bin
10       $n(M = M_{LB}) \rightarrow$  Observed number of magnitudes in the bin
11       $N_{ghost} = N(M = M_{LB}) - n(M = M_{LB}) \rightarrow$  Number of missing events
12      in the bin
13       $M = [M_{LB}] * N_{ghost} \rightarrow$  Vector of missing magnitudes in the bin
14      Update variables:
15       $M_{UB} = M_{LB}$ ;
16       $M_{LB} = M_{UB} - mbin$ ;
17       $N(M \geq M_{UB}) = N(M \geq M_{LB})$ 
18    end
19  end
20 end

```

2.5.2 Simulation of occurrence times

Occurrence times are simulated from an uniform distribution whose support are the time limits of the δk -step. As already discussed, earthquake detection rate can be assumed constant within intervals including few events, i.e within very short time intervals. The main steps are summarized in Algorithm 2.

Algorithm 2: Occurrence times simulation

```

1 for each STAI gap do
2   for each step in the gap do
3     while count  $\leq$  Number of earthquakes missing in the step do
4        $t_{i-1} =$  start time of the step;
5        $t_i =$  end time of the step;
6        $U = \text{RAND}(0,1)$ ;
7        $T = t_{i-1} + U \cdot (t_i - t_{i-1})$ ;
8       count + = 1;
9     end
10  end
11 end

```

2.5.3 Simulation of epicenter coordinates

Latitude and longitude of missing events are assigned with a probability that increases as the rate of earthquakes increases, i.e. as the distance from the large event diminishes. The rationale is based on kernel smoothing techniques, commonly implemented to forecast the density of future seismicity given the spatial distribution of past events (e.g. Frankel, 1995; Helmstetter et al., 2006; Zechar & Jordan, 2010). Specifically, a Gaussian kernel (Zechar & Jordan, 2010) is used, which is a function of the smoothing distance σ only. For each STAI gap, RESTORE extracts the pertaining subset from the catalog, that is all the events meeting the following two criteria: 1) their occurrence times range between the start and end time of the STAI gap; 2) their epicenter coordinates fall

188 within a rectangular grid representing the large shock "influence area". As a proxy for
 189 the latter, the algorithm uses the estimation of the subsurface rupture length through
 190 the relation proposed by (Mai & Beroza, 2000):

$$M_o = 10^{\frac{3}{2}(M_w + 10.7)} \cdot 10^{-7}; \quad (3)$$

$$R_l = 10^{-5.20 + 0.35 \cdot \log(M_o)} \quad (4)$$

The grid is discretized in cells, whose width depends on the bin in the latitude and longitude direction *sbin* (*sbin* = 0.01 deg in both the directions, by default). The smoothing kernel is defined as follow:

$$K_\sigma = \frac{1}{2\pi\sigma^2} \exp\left(\frac{-R^2}{2\sigma^2}\right), \quad (5)$$

191 where σ is the smoothing distance (set to 1 by default) and R is the distance of a given
 192 earthquake from a given grid node. The kernel smoothing technique offers an intuitive
 193 representation of seismicity clustering in space: as a matter of fact, events that are close
 194 in space will mainly contribute to the same (few) nodes in the grid. The events count
 195 at each grid node is estimated by summing up the contributions from all the events in
 196 the grid to that specific point. Normalizing the smoothed rate by the total rate yields
 197 the expected earthquake density over all the grid nodes. The latter is used as the basis
 198 for assigning epicenter locations to a given grid point, i.e. with a probability that is
 199 proportional to the expected earthquake rate at that location. This is achieved by simply
 200 applying the discrete version of the inverse method to the cumulative distribution
 201 of the normalized smoothed rate. Once an epicenter has been linked to a specific grid
 202 point XY , its latitude (longitude) is simulated from an uniform distribution whose support
 203 is ($[lat(XY) - sbin, lat(XY) + sbin]$ [$lon(XY) - sbin, lon(XY) + sbin$]). Main
 204 steps are summarized in Algorithm 3:

Algorithm 3: Epicenters latitude and longitudes simulation

```

input: CUMSUM: Cumulative sum of the (sorted) smoothed rate
1 for each STAI gap do
2   while count  $\leq$  Number of earthquakes missing in the STAI gap do
3     U = RAND(0,1);
4     for each grid point XY do
5       if CUMSUM(XY - 1)  $\leq$  U < CUMSUM(XY) then
6         U2 = RAND(0,1);
7         LON = LON(XY - 1) + U2 · sbin;
8         LAT = LAT(XY - 1) + U2 · sbin;
9       end
10    end
11    count + = 1;
12  end
13 end

```

2.6 Output

206
 207 RESTORE replenishes the original catalog with the reconstructed events, by properly
 208 taking into account the occurrence time of the latter. The resulting catalog is saved
 209 in ZMAP format and differs from the original one only for two aspects: 1) the depth column
 210 is now a zeros vector, as this information has not been taken into account for the
 211 spatial simulation of missing earthquakes; 2) there is an additional column which flags
 212 events to 0 or 1, depending on whether they belong to the original catalog or they have
 213 been simulated. Additionally, several graphical outputs are returned:

- 214 • Time evolution of magnitude of completeness, with highlighted all detected STAI
- 215 gaps (the plot neglects the seismic quiescent period);
- 216 • Magnitudes versus sequential numbers for the original and replenished catalogs:
- 217 this is a great, tough qualitative, tool to highlight STAI issues which could possible
- 218 affect earthquake magnitudes through time;
- 219 • Magnitude versus time for 1) the original catalog and the reconstructed events;
- 220 2) the original catalog only;
- 221 • Spatial map of the original events with overlapping reconstructed events;
- 222 • Magnitude-frequency distribution (MFD) for both the original and the replenished
- 223 catalogs.

224 Finally, the magnitude of completeness is estimated for both the original and the replen-

225 ished catalogs. This provides an additional test for validating the outputs by RESTORE:

226 intuitively, we expect the M_c estimated for the replenished catalog to be very close to

227 the pre-sequence value M_c^* . As for all the previous cases, this is done by means of the

228 Lilliefors test. However, the user should keep in mind that the statistical power of the

229 Lilliefors test (and, more in general, of the Kolmogorov-Smirnov test) greatly increases

230 with the sample size (Stallone, 2018; Marzocchi et al., 2020). It follows that for a large

231 number of events, which can be the case for the replenished catalog, the Lilliefors test

232 becomes very sensitive to even slight deviations from an exponential distribution. This

233 is not necessary ideal, since the detected departures could actually arise from magnitude

234 errors. We therefore strongly recommend to inspect the magnitude of completeness of

235 the replenished catalog by alternative methods as well, as those implemented in the ZMAP

236 software (Wiemer, 2001).

237 3 Synthetic test

As a validation test, we implement numerical modeling, which enables us to control the number of missing events and their collocation in the magnitude-time-space domain. The goal is to check whether the algorithm is capable of reconstructing this information with an acceptable degree of accuracy. First, we simulate a seismic catalog by implementing the stochastic program described in (Felzer et al., 2002), which simulates the ETAS model (Ogata, 1988) as a branching process. In the original code, earthquakes with a magnitude larger than 6.5 are modeled as planar sources. We change that by modeling all the events as point sources. We use the program to simulate a 2-years-long catalog in Southern California, with magnitudes ranging from 2 to 6.9. We leave unchanged the remaining parameters needed for the simulation as indicated in the code. The b -value is set equal to 1. Since our next step is to simulate incompleteness of after-shocks following the largest earthquake in the catalog, we select a subset of the simulated dataset, which ranges from 1 year before to 3 months after the occurrence of the largest earthquake ($M = 6.9$). After this step, the original catalog includes 11,169 events. We simulate the STAI issue for the largest event by following the approach described in (Ogata & Katsura, 2006). Specifically, earthquakes are filtered out at a magnitude-dependent rate, according to the cumulative normal distribution:

$$F(M|\mu, \sigma) = \int_{-\infty}^M \frac{1}{\sqrt{2\pi}\sigma} e^{-\frac{(x-\mu)^2}{2\sigma^2}} dx, \quad (6)$$

238 where μ and σ are constant: the first is the magnitude with a detection rate of 50%; the

239 latter is the standard deviation of the normal distribution. $F(M|\mu, \sigma)$ is the probability

240 of detection at magnitude M . See (Stallone, 2018) for more details. For our simulations,

241 we set $\mu = 3$ and $\sigma = 0.2$; we assume that the magnitude of completeness is

242 restored to the reference value 3 days after the occurrence of the large event. The catalog

243 after STAI modeling includes 7,744 events. Figure 1 shows the frequency-magnitude

244 distribution for the original (white circles) and incomplete (yellow circles) catalog, for

245 which the STAI issue has been modeled. Figure 2 plots the magnitude of events as a func-

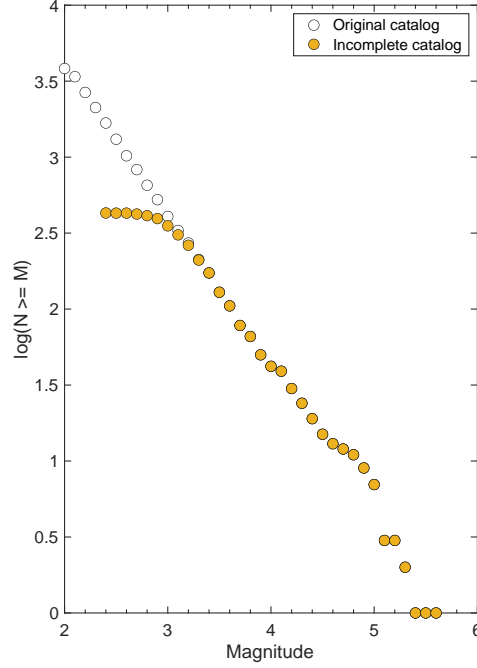


Figure 1. Frequency-magnitude distribution for the original synthetic catalog before STAI modeling (white circles) and after STAI modeling (yellow circles).

246 tion of time (over a period of 0-3 days from the mainshock) for the original (white cir-
 247 cles) and incomplete (yellow circles) catalog.

248 As a next step, we implement RESTORE for reconstructing the missing events in
 249 the magnitude-time-space domain. We leave the default values for the window size (1000
 250 events) and the step (250). The reference value for the magnitude of completeness equals
 251 the minimum magnitude in the synthetic catalog, i.e. 2.0. We set the b -value for the Gutenberg-
 252 Richter law to 1. Figure 3 shows some of the graphical outputs returned by the algorithm.
 253 We observe that occurrence times, magnitude range and locations of missing events have
 254 been correctly reconstructed. The replenished catalog includes 11,199 events, i.e. 30 events
 255 more than the original synthetic catalog. The magnitude of completeness estimated by
 256 the Lilliefors test is 2.8 and 2.1 for the incomplete and replenished catalog, respectively.
 257 In order to further inspect the algorithm performance, we compare the frequency-magnitude
 258 distribution for 1) the original synthetic catalog before STAI modeling; 2) the original
 259 synthetic catalog after STAI modeling; 3) the replenished catalog. Results are shown in
 260 Figure 4. This comparison further proves the good performance of the algorithm when
 261 reconstructing missing events in the magnitude-time-space domain.

262 4 Real-case test (Amatrice earthquake)

263 We apply RESTORE to the 24 August 2016 Mw 6.2 Amatrice earthquake. The
 264 downloaded catalog covers the period from 1st January 2016 to 30 September 2016 and
 265 includes 18,623 events. We leave the default values for the window size (1000 events) and
 266 the step (250). The seismically quiescent period ranges from 1st January 2016 to 24 Au-
 267 gust 2016 and includes 2,351 events. We estimate the reference value for the magnitude
 268 of completeness M_c^* with the Lilliefors test provided by the algorithm, which returns $M_c^* =$

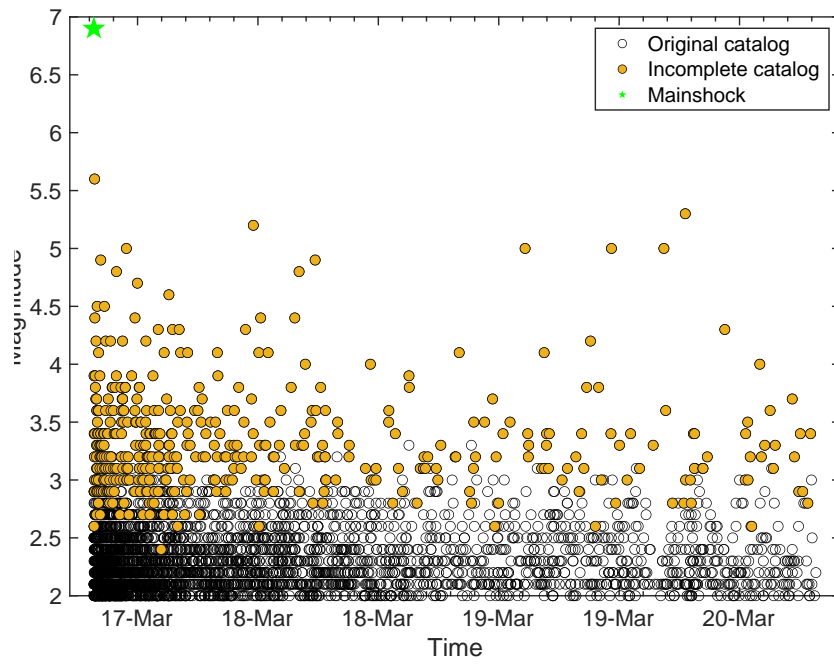


Figure 2. Magnitude-time plot for events occurred within 3 days from the large shock. White circles: before STAI modeling. Yellow circles: after STAI modeling.

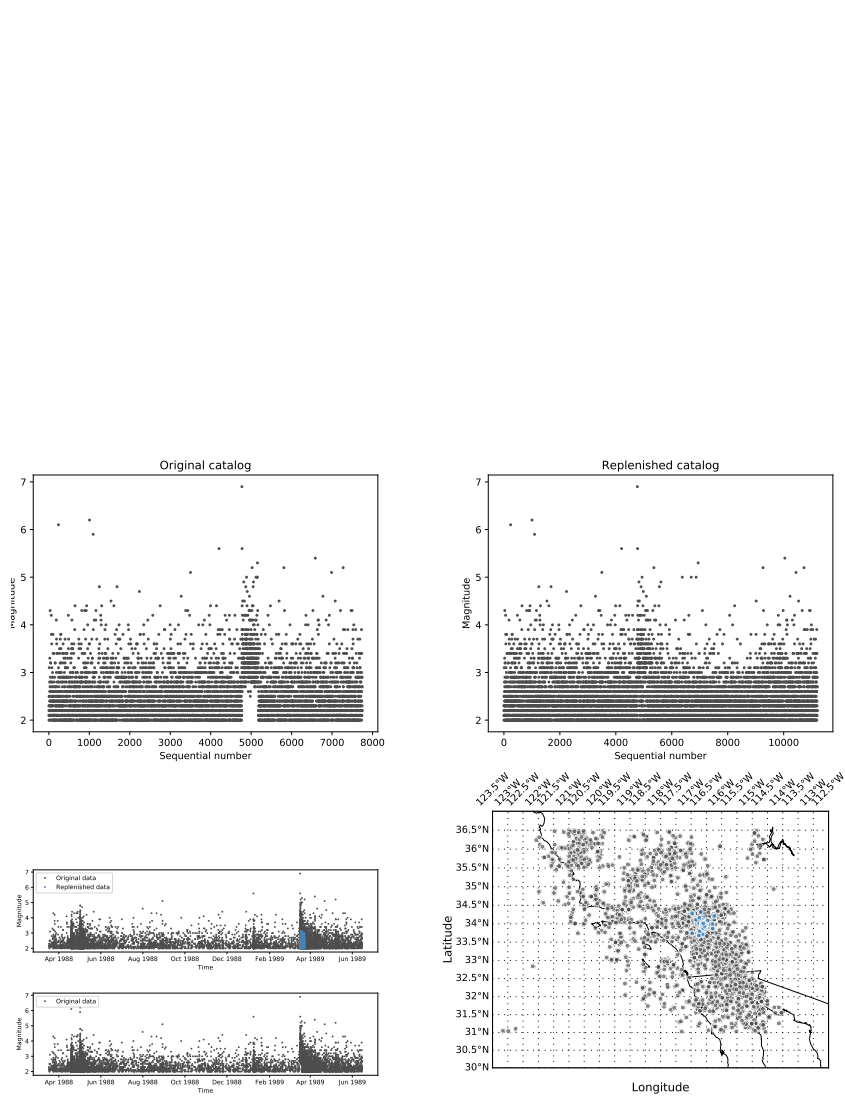


Figure 3. Main graphical outputs of the algorithm. Top Left: Magnitudes versus sequential numbers for the original (synthetic) catalog; Top Right: Magnitudes versus sequential numbers for the replenished catalog; Bottom Left: Magnitude versus time for 1) the original catalog and the reconstructed events 2) the original catalog only; Bottom Right: Spatial map of the original events with overlapping reconstructed events.

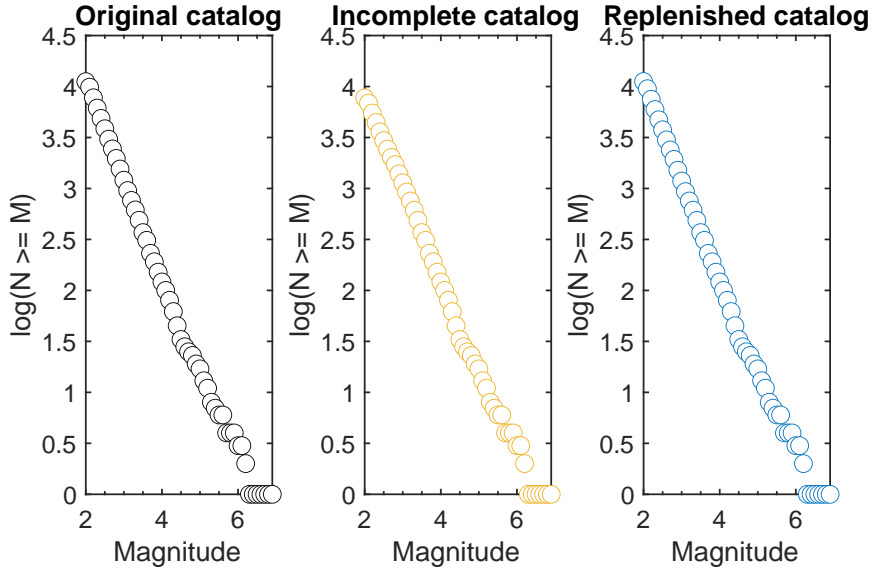


Figure 4. Frequency-magnitude distribution. From left to right: original synthetic catalog before STAI modeling, original synthetic catalog after STAI modeling, replenished catalog.

269 1.3. This leaves 11,429 earthquakes with $M \geq M_c^*$. Finally, we set the b -value for the
 270 Gutenberg-Richter law equal to 1. The replenished catalog includes 17,428 events. Fig-
 271 ure 5 plots the magnitude of completeness as a function of time, with highlighted the
 272 detected STAI gaps (four in this case). The magnitude of completeness is recovered to
 273 the reference value M_c^* after about 1 month. Figure 6 shows the other graphical outputs
 274 returned by the algorithm. While the ground truth is not known in the real-case test,
 275 we observe that the missing events are correctly reconstructed in a way which is consis-
 276 tent with data.

277 5 Conclusions

278 We have presented RESTORE, a new Python toolbox for the reconstruction of mag-
 279 nitude, time and location of events missed in the coda of large shocks. It relies on very
 280 few assumptions - e.g. the detection rate of events can be assumed to be constant within
 281 periods of time that are much shorter than the STAI extent. It also relies on a data-driven
 282 approach, which is built on well-known empirical properties of earthquake data, such as
 283 the Gutenberg-Richter law for the frequency-magnitude distribution and the aftershocks
 284 clustering in space. The critical subsets of the catalog that are affected by STAI are au-
 285 tomatically detected through a moving-window approach, which identifies statistically
 286 significant departures of the magnitude of completeness with respect to a reference value.
 287 We demonstrate the robustness of the algorithm by means of a numerical and a real-case
 288 test. In the first case, the ground truth is accurately recovered: not only the number of
 289 missing earthquakes is correctly retrieved, but their space-time-magnitude stochastic dis-
 290 tribution is correctly resolved as well. The real-test case, which applies to the Mw 6.2
 291 Amatrice earthquake, further proves the good performance of the algorithm, which re-
 292 constructs the missed events in a way that is consistent with the data. The main advan-
 293 tage of RESTORE lies in its fully data-driven approach. However, this could also rep-
 294 resent a drawback if the following aspects are not carefully taken into consideration:

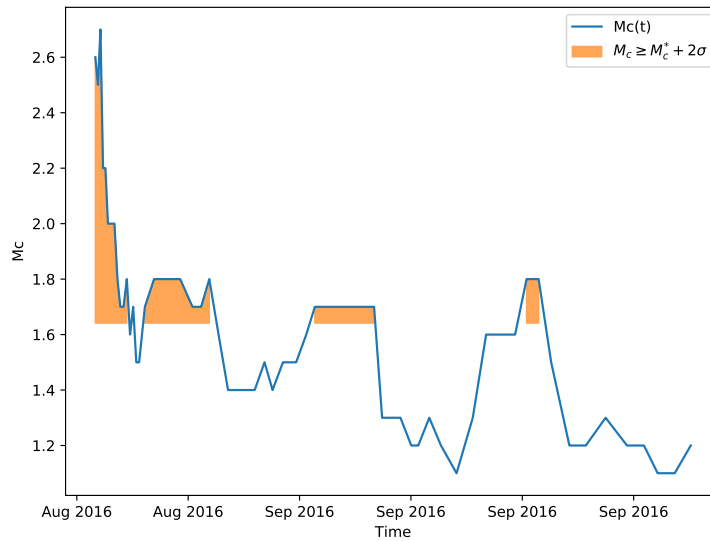


Figure 5. Temporal evolution of the magnitude of completeness, with highlighted the detected STAI gaps. The moving-window includes 1000 events and is shifted by 250 events.

- 295
- 296
- 297
- 298
- 299
- 300
- 301
- 302
- 303
- 304
- 305
- 306
- 307
- 308
- 309
- 310
- 311
- the quality of the seismic catalog: strong uncertainties about the earthquake parameters (epicenter coordinates, magnitude, occurrence time) will affect the properties of the simulated events;
 - the seismic quiescent period: it must be carefully selected for an accurate estimation of the reference value of the magnitude of completeness. Furthermore, it must be long enough to include a number of events which must be substantially higher than the chosen window size; for an unbiased estimation of M_c^* , the user is required to select the quiescent period so to include a number of events N which is a multiple of the selected window size k (we recommend at least $N \simeq 4 * k$);
 - spatial map domain: the same reasoning for the seismic quiescent period applies here as well; the selected area should obviously include the large shock/s and, at the same time, enough events in the seismic quiescent period;
 - the window size and step: the output provided by RESTORE will be affected by the values provided for these parameters; we recommend to test several alternatives and opt for those assuring the best replenishment. As detailed in the text, too small values for the size and step will likely bias the M_c estimate, whereas too large values will shadow short-term fluctuations of M_c .

312 RESTORE is made freely available and can be downloaded at the link provided in the
 313 Acknowledgments. It promises to become a valuable research tool to tackle the STAI is-
 314 s-
 315 s-
 316 s-

317 6 Data Availability Statement

318 The algorithm RESTORE is available at the following Zenodo repository: [https://](https://doi.org/10.5281/zenodo.3952182)
 319 doi.org/10.5281/zenodo.3952182, and can also be downloaded from GitHub at this

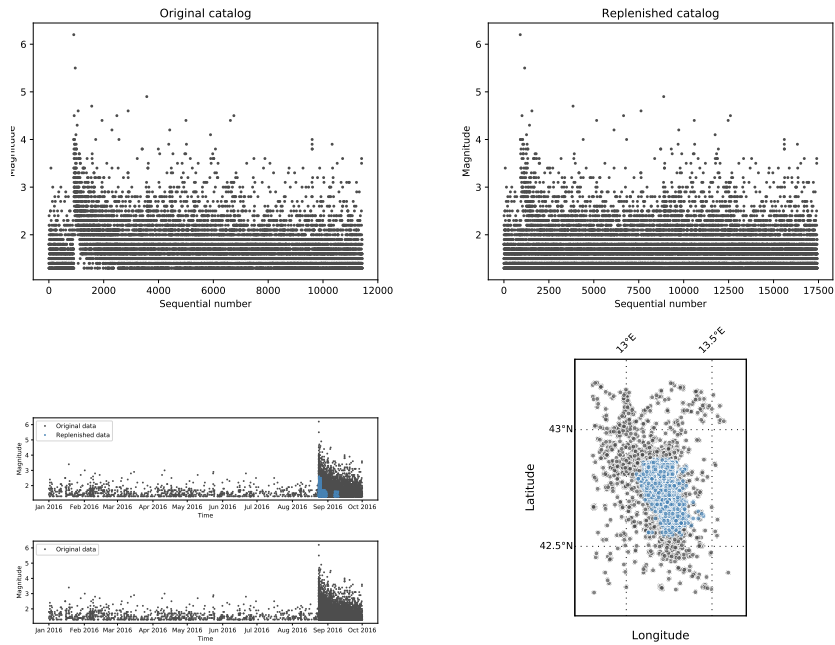


Figure 6. Main graphical outputs of the algorithm. Top Left: Magnitudes versus sequential numbers for the original catalog; Top Right: Magnitudes versus sequential numbers for the replenished catalog; Bottom Left: Magnitude versus time for 1) the original catalog and the reconstructed events 2) the original catalog only; Bottom Right: Spatial map of the original events with overlapping reconstructed events.

320 link: <https://github.com/angystallone/RESTORE>. The repository includes the dataset
 321 used for the synthetic test as well. The seismic catalog used for the real-case test (Am-
 322 atrice earthquake) is the HOMogenized instrUMENTal Seismic catalog (HORUS) of Italy
 323 (Lolli et al., 2020) and it can be downloaded at this link: <https://horus.bo.ingv.it/>.
 324 The routine *Mc-Lilliefors* implemented in RESTORE for the magnitude of complete-
 325 ness estimation is available at the following Zenodo repository: [https://doi.org/10](https://doi.org/10.5281/zenodo.4162496)
 326 [.5281/zenodo.4162496](https://doi.org/10.5281/zenodo.4162496).

327 Acknowledgments

328 This project has been funded by the Seismic Hazard Center (Centro di Pericolosità
 329 Sismica, CPS, at the Istituto Nazionale di Geofisica e Vulcanologia, INGV).

330 Appendix A Calculation of number of missing events

Here we derive Equation 1 in the text. The frequency-magnitude distribution of earthquakes is typically described by the Gutenberg-Richter (G-R) exponential law (Gutenberg & Richter, 1944):

$$N(M) = 10^{a-bM}, \quad (\text{A1})$$

331 where $N(M)$ is the number of events with magnitude above M ($M \geq M_{min}$, i.e. the
 332 minimum magnitude in the earthquake catalog), a is a constant related to the total seis-
 333 mic rate and b is the b -value, controlling the relative number of large earthquakes in the
 334 catalog. Let us consider the case where $M_2 \geq M_1$. We have:

$$\begin{aligned} N(M \geq M_1) &= 10^{a-bM_1} \\ N(M \geq M_2) &= 10^{a-bM_2} \end{aligned}$$

We start by expressing $N(M \geq M_1)$ as a function of $N(M \geq M_2)$ and b only, by calculating the ratio:

$$\frac{N(M \geq M_1)}{N(M \geq M_2)} = 10^{-b(M_1-M_2)} \quad (\text{A2})$$

This simple trick enables us to rescale the problem, i.e. to get rid of the term 10^a , which is related to the total seismic rate:

$$N(M \geq M_1) = N(M \geq M_2) \cdot 10^{-b(M_1-M_2)} \quad (\text{A3})$$

We observe that $M_2 = M_1 + n \cdot mbin$, where $mbin$ is the magnitude binning (usually equal to 0.1). It follows that:

$$N(M \geq M_1) = N(M \geq M_2) \cdot 10^{b \cdot n \cdot mbin} \quad (\text{A4})$$

For one bin only (i.e., $n = 1$):

$$N(M \geq M_1) = N(M \geq M_2) \cdot 10^{b \cdot mbin} \quad (\text{A5})$$

335 This equation allows to retrieve the number of expected events with magnitude $M \geq$
 336 M_1 as a function of the number of events with magnitude $M \geq M_2$. In other words,
 337 we can extrapolate the frequency of earthquakes above a given magnitude to any lower
 338 magnitude cutoff. Note that we implicitly assume the b -value is constant for any sub-
 339 set of the whole catalog.

340 References

341 Brodsky, E. (2011). The spatial density of foreshocks. *Geophysical Research Letters*,
 342 *38*(10).

- 343 Christophersen, A., & Smith, E. G. (2008). Foreshock rates from aftershock abun-
 344 dance. *Bulletin of the Seismological Society of America*, *98*(5), 2133–2148.
- 345 Clauset, A., Shalizi, C. R., & Newman, M. E. (2009). Power-law distributions in em-
 346 pirical data. *SIAM review*, *51*(4), 661–703.
- 347 Devroye, L. (1986). Sample-based non-uniform random variate generation. In *Pro-*
 348 *ceedings of the 18th conference on winter simulation* (pp. 260–265).
- 349 Efron, B. (1992). Bootstrap methods: another look at the jackknife. In *Break-*
 350 *throughs in statistics* (pp. 569–593). Springer.
- 351 Enescu, B., Mori, J., & Miyazawa, M. (2007). Quantifying early aftershock activity
 352 of the 2004 mid-niigata prefecture earthquake (mw6. 6). *Journal of Geophys-*
 353 *ical Research: Solid Earth*, *112*(B4).
- 354 Enescu, B., Mori, J., Miyazawa, M., & Kano, Y. (2009). Omori-utsu law c-values as-
 355 sociated with recent moderate earthquakes in japan. *Bulletin of the Seismolog-*
 356 *ical Society of America*, *99*(2A), 884–891.
- 357 Felzer, K. R., Becker, T. W., Abercrombie, R. E., Ekström, G., & Rice, J. R. (2002).
 358 Triggering of the 1999 mw 7.1 Hector mine earthquake by aftershocks of the
 359 1992 mw 7.3 Landers earthquake. *Journal of Geophysical Research: Solid*
 360 *Earth*, *107*(B9), ESE–6.
- 361 Felzer, K. R., Page, M. T., & Michael, A. J. (2015). Artificial seismic acceleration.
 362 *Nature Geoscience*, *8*(2), 82–83.
- 363 Frankel, A. (1995). Mapping seismic hazard in the central and eastern united states.
 364 *Seismological Research Letters*, *66*(4), 8–21.
- 365 Gutenberg, B., & Richter, C. F. (1944). Frequency of earthquakes in california. *Bul-*
 366 *letin of the Seismological Society of America*, *34*(4), 185–188.
- 367 Hainzl, S., Zakharova, O., & Marsan, D. (2013). Impact of aseismic transients on the
 368 estimation of aftershock productivity parameters. *Bulletin of the Seismological*
 369 *Society of America*, *103*(3), 1723–1732.
- 370 Helmstetter, A., Kagan, Y. Y., & Jackson, D. D. (2005). Importance of small earth-
 371 quakes for stress transfers and earthquake triggering. *Journal of Geophysical*
 372 *Research: Solid Earth*, *110*(B5).
- 373 Helmstetter, A., Kagan, Y. Y., & Jackson, D. D. (2006). Comparison of short-term
 374 and time-independent earthquake forecast models for southern california. *Bul-*
 375 *letin of the Seismological Society of America*, *96*(1), 90–106.
- 376 Herrmann, M., & Marzocchi, W. (2020a). Inconsistencies and lurking pitfalls in the
 377 magnitude–frequency distribution of high-resolution earthquake catalogs. *Seis-*
 378 *mological Research Letters*.
- 379 Herrmann, M., & Marzocchi, W. (2020b, November). *Mc-Lilliefors: a completeness*
 380 *magnitude that complies with the exponential-like Gutenberg–Richter relation*.
 381 Zenodo. Retrieved from <https://doi.org/10.5281/zenodo.4162497> doi:
 382 10.5281/zenodo.4162497
- 383 Iwata, T. (2008). Low detection capability of global earthquakes after the occurrence
 384 of large earthquakes: Investigation of the harvard cmt catalogue. *Geophysical*
 385 *Journal International*, *174*(3), 849–856.
- 386 Kagan, Y. Y. (2004). Short-term properties of earthquake catalogs and models
 387 of earthquake source. *Bulletin of the Seismological Society of America*, *94*(4),
 388 1207–1228.
- 389 Kagan, Y. Y. (2013). *Earthquakes: models, statistics, testable forecasts*. John Wiley
 390 & Sons.
- 391 Knopoff, L., Kagan, Y. Y., & Knopoff, R. (1982). b values for foreshocks and after-
 392 shocks in real and simulated earthquake sequences. *Bulletin of the Seismologi-*
 393 *cal Society of America*, *72*(5), 1663–1676.
- 394 Lilliefors, H. W. (1969). On the kolmogorov-smirnov test for the exponential dis-
 395 tribution with mean unknown. *Journal of the American Statistical Association*,
 396 *64*(325), 387–389.

- 397 Lippiello, E., Godano, C., & de Arcangelis, L. (2012). The earthquake magnitude is
 398 influenced by previous seismicity. *Geophysical Research Letters*, *39*(5).
- 399 Loli, B., Randazzo, D., Vannucci, G., & Gasperini, P. (2020). The homogenized in-
 400 strumental seismic catalog (horus) of italy from 1960 to present. *Seismological*
 401 *Society of America*, *91*(6), 3208–3222.
- 402 Mai, P. M., & Beroza, G. C. (2000). Source scaling properties from finite-fault-
 403 rupture models. *Bulletin of the Seismological Society of America*, *90*(3), 604–
 404 615.
- 405 Marzocchi, W., Spassiani, I., Stallone, A., & Taroni, M. (2020). How to be fooled
 406 searching for significant variations of the b-value. *Geophysical Journal Interna-*
 407 *tional*, *220*(3), 1845–1856.
- 408 Mignan, A., & Woessner, J. (2012a). Estimating the magnitude of completeness
 409 for earthquake catalogs. *Community Online Resource for Statistical Seismicity*
 410 *Analysis*, 1–45.
- 411 Mignan, A., & Woessner, J. (2012b). *Theme iv—understanding seismicity cat-*
 412 *alogs and their problems* (Tech. Rep.). Technical Report doi: [https://doi.](https://doi.org/10.5078/corssa-00180805)
 413 [org/10.5078/corssa-00180805](https://doi.org/10.5078/corssa-00180805), Community
- 414 Ogata, Y. (1988). Statistical models for earthquake occurrences and residual
 415 analysis for point processes. *Journal of the American Statistical association*,
 416 *83*(401), 9–27.
- 417 Ogata, Y. (1998). Space-time point-process models for earthquake occurrences. *An-*
 418 *nals of the Institute of Statistical Mathematics*, *50*(2), 379–402.
- 419 Ogata, Y., & Katsura, K. (1993). Analysis of temporal and spatial heterogeneity
 420 of magnitude frequency distribution inferred from earthquake catalogues. *Geo-*
 421 *physical Journal International*, *113*(3), 727–738.
- 422 Ogata, Y., & Katsura, K. (2006). Immediate and updated forecasting of aftershock
 423 hazard. *Geophysical research letters*, *33*(10).
- 424 Omi, T., Ogata, Y., Hirata, Y., & Aihara, K. (2013). Forecasting large aftershocks
 425 within one day after the main shock. *Scientific reports*, *3*, 2218.
- 426 Omi, T., Ogata, Y., Hirata, Y., & Aihara, K. (2014). Estimating the etas model
 427 from an early aftershock sequence. *Geophysical Research Letters*, *41*(3), 850–
 428 857.
- 429 Peng, Z., Vidale, J. E., & Houston, H. (2006). Anomalous early aftershock decay
 430 rate of the 2004 mw6. 0 parkfield, california, earthquake. *Geophysical Research*
 431 *Letters*, *33*(17).
- 432 Peng, Z., Vidale, J. E., Ishii, M., & Helmstetter, A. (2007). Seismicity rate imme-
 433 diately before and after main shock rupture from high-frequency waveforms in
 434 japan. *Journal of Geophysical Research: Solid Earth*, *112*(B3).
- 435 Peng, Z., & Zhao, P. (2009). Migration of early aftershocks following the 2004 park-
 436 field earthquake. *Nature Geoscience*, *2*(12), 877–881.
- 437 Schorlemmer, D., Neri, G., Wiemer, S., & Mostaccio, A. (2003). Stability and signif-
 438 icance tests for b-value anomalies: Example from the tyrrhenian sea. *Geophys-*
 439 *ical research letters*, *30*(16).
- 440 Seif, S., Mignan, A., Zechar, J. D., Werner, M. J., & Wiemer, S. (2017). Estimating
 441 etas: The effects of truncation, missing data, and model assumptions. *Journal*
 442 *of Geophysical Research: Solid Earth*, *122*(1), 449–469.
- 443 Stallone, A. (2018). *Statistical analysis of earthquake occurrences and implications*
 444 *for earthquake forecasting and seismic hazard assessment* (Doctoral disserta-
 445 tion, University of Roma TRE). doi: 10.13140/RG.2.2.35672.65282/1
- 446 Stallone, A., & Marzocchi, W. (2019). Empirical evaluation of the magnitude-
 447 independence assumption. *Geophysical Journal International*, *216*(2), 820–
 448 839.
- 449 Wiemer, S. (2001). A software package to analyze seismicity: Zmap. *Seismological*
 450 *Research Letters*, *72*(3), 373–382.
- 451 Woessner, J., Laurentiu, D., Giardini, D., Crowley, H., Cotton, F., Grünthal, G., . . .

- 452 others (2015). The 2013 european seismic hazard model: key components and
453 results. *Bulletin of Earthquake Engineering*, *13*(12), 3553–3596.
- 454 Woessner, J., & Wiemer, S. (2005). Assessing the quality of earthquake catalogues:
455 Estimating the magnitude of completeness and its uncertainty. *Bulletin of the*
456 *Seismological Society of America*, *95*(2), 684–698.
- 457 Zechar, J. D., & Jordan, T. H. (2010). Simple smoothed seismicity earthquake fore-
458 casts for italy. *Annals of Geophysics*, *53*(3), 99–105.
- 459 Zhuang, J., Ogata, Y., & Wang, T. (2017). Data completeness of the kumamoto
460 earthquake sequence in the jma catalog and its influence on the estimation of
461 the etas parameters. *Earth, Planets and Space*, *69*(1), 36.
- 462 Zhuang, J., Wang, T., & Koji, K. (2019). Detection and replenishment of missing
463 data in marked point processes.. Retrieved from [http://bemlar.ism.ac.jp/
464 zhuang/pubs/zhuang2019statsini.pdf](http://bemlar.ism.ac.jp/zhuang/pubs/zhuang2019statsini.pdf)